Fermi National Accelerator Laboratory

FN-436
0302.000

# SPACE-CHARGE EFFECTS OF TRANSITION CROSSING IN THE FERMILAB BOOSTER

King-Yuen Ng

Fermi National Accelerator Laboratory, Batavia, Illinois 60510

September 1986

Operated by Universities Research Association Inc. under contract with the United States Department of Energy

FN-436
0302.000

September, 1986

# SPACE-CHARGE EFFECTS OF TRANSITION CROSSING IN THE FERMILAB BOOSTER

King-Yuen Ng
*Fermi National Accelerator Laboratory, Batavia, IL 60510*

**Abstract**

The bunch area increases after crossing transition. This is found to be due to space-charge distortion of the RF rather than microwave instability. The possibility of a $\gamma_t$ jump is investigated.

# I Introduction

The bunch area of a typical bunch in the booster across transition had been measured by J. Crisp[1] and is shown in Fig. 1. (Here, the bunch area is defined as the bucket area multiplied by square of the ratio of the bunch length to the bucket length). We see that the bunch area is roughly constant before transition but increases abruptly after transition. The mountain-range plots of Fig. 2 measured by Crisp[1] reveal quadrupole oscillations of bunch after transition. This implies that the growth in bunch area may not be a result of microwave instability but is due to space-charge effects which make the bunch tumble in the bucket after transition. The physics of this space-charge effect is discussed in Section II. The equations of motion governing the tumbling are reviewed in Section III. Comparisons of the theoretical computations to the mountain-range measurements are done in Section IV. The agreement turns out to be very satisfactory. In Section V, microwave instability is discussed. In Section VI, the methods of triple-phase switch and $\gamma_t$ jump are discussed to cure the bunch tumbling. It turns out that $\gamma_t$ jump is the best method to avoid the growth of bunch area across transition. However, the position of the jump is very essential to the cancelling of the tumbling.

# II Physics of Space-Charge Tumbling

The space-charge force increases the energy of particles at the front of a bunch and decrease the energy of those at the rear end. Thus, below transition, the bunch is longer than if space charge is not present and is shorter above transition. A plot of the equilibrium bunch length is shown in Fig. 3 where $\theta$ is the normalized bunch length in RF radians, $x$ the normalized time (0 at transition) and $\eta_0$ is the ratio of the space-charge force to the linearized RF force. All these variables are explained in Section III.

With space charge, if a bunch fits the bucket below transition, its length will have to be shortened after transition in order to fit the bucket after transition. But in doing so, the length will generally overshoot (become too short) and will therefore oscillate about the equilibrium bunch length as shown in Fig. 4. This is just the tumbling of an elongated bunch inside a bucket.

# III Equations of Motion

The mathematics of a parabolic bunch in a linearized RF voltage had been studied in detail by Sorenssen[2]. Here, we merely quote the equations of motion and give definitions of the necessary parameters.

Assume that the RF voltage $V_{RF}$ is linearized, the RF phase $\varphi_0$ (or $\pi - \varphi_0$) are held constant over a time period including point of transition, and the frequency-flip parameter per unit particle energy $\eta/E$ varies as a linear function of time. The equations of motion are:

$$\frac{d\theta}{dx} = xP, \tag{1}$$

$$\frac{dP}{dx} = -sgn\left[(x-x_1)(x-x_2)(x-x_3)\right]\theta - \frac{0.7723\eta_0}{\theta^2} + \frac{x}{\theta^3}, \tag{2}$$

where $\theta(x)$ is the normalized half width of a parabolic bunch and $P(x)$ its canonical variable. The normalized half height $p(x)$ of the bunch is given by $(P^2 + \theta^{-2})^{1/2}$. The normalized time $x$ is measured in units of the characteristic time $T$ given by

$$T = \left[\left(\frac{\gamma_t^4}{2\dot{\gamma}_t h\omega_\infty^2}\right)\left(\frac{2\pi E_0}{eV_{RF}\left|\cos\varphi_0\right|}\right)\right]^{\frac{1}{3}}. \tag{3}$$

In above, $E_0 = m_p c^2$ is the energy of the proton at rest, $\omega_\infty$ is the angular revolution frequency of a particle around the ring travelling with the velocity of light $c$, $h$ the RF harmonic,

$$\dot{\gamma}_t = \frac{eV_{RF}\sin\varphi_0\omega_\infty\beta_t}{2\pi E_0}, \tag{4}$$

and $\beta_t c$ is the particle velocity at transition. Note that $T$ depends on $V_{RF}$ and $\varphi_0$ only and is independent of the bunch intensity. The characteristic time $T$ is the time around transition when the evolution is not adiatbatic. The symbols $x_1, x_2, x_3$ in Eq. (2) allow for three possible time moments when the RF phase $\varphi_0$ is switched to $\pi - \varphi_0$, then back to $\varphi_0$ and to $\pi - \varphi_0$ again.

The normalized half bunch length $\theta$ is related to the true half bunch length $\hat{\theta}$ by $\hat{\theta} = (3/\pi)^{1/2}A\theta$, where, with the bunch area $S$ in eV-sev,

$$A = \left(\frac{2\dot{\gamma}_t S}{3E_0}\right)^{\frac{1}{2}}\left(\frac{h\omega_\infty T}{\gamma_t^2}\right). \tag{5}$$

The normalized half bunch height $p$ is related to the maximum half bunch height $\Delta\hat{E}/E$ by

$$\frac{\Delta\hat{E}}{E} = \left(\frac{3}{\pi}\right)^{\frac{1}{2}}\left(\frac{\Gamma A}{\gamma_t}\right)p(x), \tag{6}$$

where

$$\Gamma = \left(\frac{eV_{RF}\beta_t^2\gamma_t^4\cos^2\varphi_0}{4\pi h E_0\sin\varphi_0}\right)^{\frac{1}{3}}. \tag{7}$$

The rate of increase in energy of a particle due to the linearized RF is

$$\dot{E}_{RF} = \frac{eV_{RF}\omega \left|\cos\varphi_0\right|}{2\pi}\Delta\varphi, \tag{8}$$

where $\omega = \beta_t \omega_\infty$ is the angular revolution frequency and $\Delta\varphi$ is the deviation of the RF phase from that of the synchronous particle. The rate of increase in energy due to space-charge force is

$$\dot{E}_{sc} = -\frac{e^2 g_0 \omega h^2}{4\pi\epsilon_0 R\gamma^2}\frac{\partial\lambda}{\partial\Delta\varphi}, \tag{9}$$

where $g_0 = 2\ln(b/a)+1$ is the familiar space-charge geometric factor ($a$ and $b$ being the radii of the beam and the beam pipe respectively), $R$ the mean radius of the booster ring, and $\lambda(\Delta\varphi) = (3N/h\hat{\theta}^3)(\hat{\theta}^2 - \Delta\varphi^2)$ is the linear density of one parabolic bunch with half length $\hat{\theta}$ and containing $N/h$ particles. The total rate of energy increase can therefore be written as

$$\dot{E} = \frac{eV_{RF}\omega \left|\cos\varphi_0\right|}{2\pi}\left(1+\eta_{sc}\right)\Delta\varphi, \tag{10}$$

where we have introduced the space-charge parameter $\eta_{sc}$ which is defined as the ratio of the space-charge force to the RF force. Since $\eta_{sc}$ depends on the instantaneous bunch length $\hat{\theta}^3$ which is a function of time and space charge, we can normalize $\eta_{sc}$ by replacing $\hat{\theta}$ by $\hat{\theta}_0$, the bunch length at transition *without* space charge, or

$$\eta_{sc} = \eta_0 \left(\frac{\hat{\theta}_0}{\hat{\theta}}\right)^3. \tag{11}$$

Writing it out explicitly, we have

$$\eta_0 = \frac{1}{2}\left(\frac{3}{2}\right)^{\frac{1}{2}}\left(\frac{\pi}{\Gamma(\frac{2}{3})}\right)^3\left(\frac{r_p N g_0 E_0^2}{hcS^{3/2}}\right)\left(\frac{2\pi}{eV_{RF}\sin\varphi_0\omega}\right)^{\frac{1}{2}}, \tag{12}$$

where $r_p = 1.5347 \times 10^{-16}$ cm is the classical proton radius. This space-charge parameter $\eta_0$ is the only parameter in the equations of motion (1) and (2). Thus, with the normalized quantities, the equations of motion are, in fact, universal for all machines.

The equations are solved numerically with the initial condition that the bunch is matched to the bucket far before transition. A distortion parameter $D$ is introduced to measure the elongation of the bunch or the distortion from the equilibrium bunch shape. It is defined as the square root of the ratio of the maximum to minimum bunch lengths. Note that, with space charge, the bunch is not a right ellipse, so that $D(x)$ cannot be exactly equal to unity even away from transition. In the plot, the $D$ quoted is its value at $x = 15$ and $D(0)$ is the value without space charge.

# IV Comparision with Mountain-Range Measurements

Three different mountain-range measurements were taken and are shown in Fig. 2. The RF phase was flipped right at transition, 0.2 ms and 0.4 ms after transition respectively in the three measurements. But only one flip was performed in each case. In the plots, each successive trace represents a lapse of ten turns.

For the measurement, the data are: total number of particles $N = 1.30 \times 10^{12}$, RF voltage $V_{RF} = 763$ kV, RF phase $\varphi_0 = 53.6°$, RF harmonic $h = 84$, longitudinal bunch area $S = 0.025$ eV-sec, $\gamma_t = 5.373$, and revolution frequency $\omega_\infty = 3.972 \times 10^6$ Hz. Thus, the rate of change of $\gamma$ at transition is $\dot{\gamma}_t = 406.5$ sec$^{-1}$ and the characteristic time is $T = 0.2160$ ms. The space-charge parameter is $\eta_0 = 0.2183\, g_0$. Since the space-charge geometical factor is usually $g_0 \sim 4.5$, we take $\eta_0 = 1.00$. From Eq. (5), the true half bunch length $\hat{\theta}$ is related to the normalized half length $\theta$ by

$$\hat{\theta} = 0.2073\, \theta. \tag{13}$$

Numerical computations are then made with transition crossing at $x_1 = x_2 = x_3 = 0$, $0.2/0.216 = 0.925$, and $0.4/0.216 = 1.85$ respectively. The results are shown in Figs. 4, 5, and 6. They are then compared with the experimental measurements.

## IV-1 First performance, RF phase switched at $t = 0$.

The comparison is shown in Table 1. In general, the agreement of experimental

| | Experimental | | | Theoretical | | |
|---|---|---|---|---|---|---|
| | trace number | time (ms) | half length (RF rad) | $x$ | $t = xT$ (ms) | half length (RF rad) |
| transition | 23 | 0.00 | 0.24 | 0.00 | 0.00 | 0.23 |
| 1st min. | 43 | 0.32 | | 1.40 | 0.30 | |
| 1st max. | 60 | 0.60 | 0.42 | 2.56 | 0.55 | 0.52 |
| 2nd min. | 72 | 0.79 | | 3.40 | 0.73 | |
| 2nd max. | 83 | 0.97 | 0.49 | 0.42 | 0.91 | 0.59 |
| 3rd min. | 94 | 1.14 | | 4.91 | 1.06 | |
| 3rd max. | 104 | 1.30 | 0.53 | 5.59 | 1.21 | 0.64 |
| 4th min. | 113 | 1.45 | | 6.21 | 1.34 | |
| 4th max. | 122 | 1.59 | 0.56 | 6.82 | 1.47 | 0.72 |

Table 1: Bunch lengths comparison for first performance.

results with theory is quite good. A more careful look reveals that the experimental oscillation periods are consistently 8% bigger than the theoretical predictions. Also the experimental half bunch lengths are smaller. The positions of the maxima and minima are not sensitive to $\eta_0$. For example, even if we lower $\eta_0$ from 1 to 0.25, the position of the 4th maximum changes from $x = 6.82$ to only 7.0, which is not big enough to match the experimental results. The main reason of the discrepancy is due to the linearization of the RF force in Eqs. (1) and (2). In fact, the bunch fills up a very large part of the accelerating bucket. This makes the average synchrotron period longer and the bunch length shorter.

The two ends of the accelerating bucket $\phi_1$ and $\phi_2$ are given by

$$\phi_2 \sin\varphi_0 + \cos\phi_2 = \phi_1 \sin\varphi_0 - \cos\varphi_0, \tag{14}$$

where $\phi_1 = \pi - \varphi_0$. Above transition, $\varphi_0 = 180° - 53.6° = 2.21$ rad. Thus $\phi_1 = 0.94$ rad and $\phi_2 = 2.87$ rad. In the fish-shaped moving bucket, the short side of the half bucket length is therefore $\phi_2 - \varphi_0 = 0.66$ rad. On the other hand, the half length of the bunch is 0.56 rad for the 4th maximum. Thus, the elongated bunch is quite close to the edge of the bucket. This also explains why filamentation was observed just a couple of synchrotron oscillations ($\sim 2.7$ ms) after transition.

## IV-2 Second performance, RF phase switched at 0.20 ms.

The experimental traces show an apparent split in the bunch just after transition. This is not shown in the numerical solution of Fig. 5. This may be due to modification of the RF potential by other effects (for example, wall impedance) other than space charge or microwave growth discussed in the next section. Since the origin of the split is not clear, no comparison with theory is attempted.

## IV-3 Third performance, RF phase switched at 0.40 ms.

The comparison is shown in Table 2. Here, the experimental results exhibit no first minimum which agree with the theoretical prediction. Again the positions of maxima and minima are consistently bigger for the experimental results and this is due to a tight bucket which gives a lower average oscillation rate. The predicted maximum half lengths are too big. Of course, this is due mostly to the linearization of the RF force. However, they are very sensitive to the time at which the RF phase is switched. An earlier switch will lower these maxima by very much.

Since the agreement between experimental measurements and theory, at least for the first and third performances, we may conclude that the growth in bunch area

| | Experimental | | | Theoretical | | |
|---|---|---|---|---|---|---|
| | trace number | time (ms) | half length (RF rad) | $x$ | $t = xT$ (ms) | half length (RF rad) |
| transition | 23 | 0.00 | 0.23 | 0.00 | 0.00 | 0.23 |
| 1st max. | 60 | 0.60 | 0.62 | 2.54 | 0.53 | 1.40 |
| 1st min. | 72 | 0.79 | | 3.35 | 0.72 | |
| 2nd max. | 84 | 0.98 | 0.72 | 4.17 | 0.90 | 1.59 |
| 2nd min. | 95 | 1.16 | | 4.89 | 1.06 | |
| 3rd max. | 106 | 1.34 | 0.72 | 5.59 | 1.21 | 1.64 |
| 3rd min. | 115 | 1.48 | | 6.26 | 1.35 | |
| 4th max | 124 | 1.63 | 0.72 | 6.85 | 1.48 | 1.85 |

Table 2: Bunch lengths comparision for third performance.

across transition is due mostly to space-charge effects which lead to bunch tumbling inside the bucket and eventual filamentation.

# V Microwave Instability

The equations of motion (1) and (2) originate from a set of linear equations for any single particle in the bunch:

$$\frac{d}{dt}\begin{pmatrix} \tilde{\theta} \\ \tilde{p} \end{pmatrix} = \begin{pmatrix} F_1 & F_2 \\ F_3 & F_4 \end{pmatrix}\begin{pmatrix} \tilde{\theta} \\ \tilde{p} \end{pmatrix}, \tag{15}$$

where $\tilde{\theta}$ and $\tilde{p}$ are canonical variables denoting the particle's position in the longitudinal phase space. The coefficents $F_1, F_2, F_3, F_4$ are independent of $\tilde{\theta}$ and $\tilde{p}$, although they do depend on time and the bunch length $\hat{\theta}$ at that time. Since the equations are linear, the evolution of the position particle can therefore be obtained by successive linear transformations. Thus, a parabolic bunch will remain parabolic for ever and no change in bunch area will result. For this reason, our computation will *not* include any microwave instability which will lead to growth in bunch area. So only a qualitative discussion is given here.

After passing through transition, space-charge force inevitably leads to microwave instability. However, usually the worst growth will appear only during the first few units of the characteristic time T. Figures 7, 8, 9 show the energy half spreads when the RF phases are switched at $x = 0.0, 0.93$ and $1.85$ (or $t = 0.0, 0.20, 0.40$ ms) respectively. Both Figs. 7 and 9, display, during the first few units of T, energy spreads which are much bigger than that when there is no space charge. As a result, the oscillations after transition do lower the growth of the microwave amplitudes and therefore the bunch area, although we do not know how to relate the two growths. When the RF phase is switched at $x = 0.93$ (or $t = 0.20$ ms), we do not see the big energy-spread peak just after transition (Fig. 8). As a result, the microwave growth is expected to be bigger. This may explain why the experimental data shows a split bunch (Fig. 2).

# VI Cures of Bunch Tumbling

Here, we try to evaluate three methods to cure bunch tumbling.

## VI-1 Triple-phase switch

Sorensen[2] suggested switching the RF phase back and forth three times to damp out the oscillations after transition. The idea is as follows: after switching the phase from $\varphi_0$ to $\pi - \varphi_0$ at $x_1 = 0$, the bunch tries to adjust itself to fit the configuration of shorter bunch length (Fig. 4). But it will usually overshoot. At some time $x_2$ before the overshoot, the phase is switched from $\pi = \varphi_0$ to $\phi_0$. The bunch is then at an unstable fixed point and it will try to lengthen. Then, the phase is switched back to $\pi - \varphi_0$ at $x_3$. Proper times $x_2$ and $x_3$ are so chosen that the bunch lengthening between this interval will cancel the overshoot thus damping out the oscillations and eventual filamentation.

With $\eta_0 = 1$, we find a set of time $x_2 = 0.688$ and $x_3 = 1.289$ that will cancel the overshoot. The distortion factor is reduced from the original $D = 1.72$ to $D = 1.03$ (Fig. 10). The defination of $D$ is given in Section III. There are many possible sets $x_2$ and $x_3$. If we want to damp the oscillation by cancelling the second overshoot, we can choose $x_2 = 2.96$ and $x_3 = 3.29$. The distortion is then $D = 1.03$.

However, this method will not work well for the following reasons:

(1) The best moment to damp the oscillations is to cancel the first overshoot in order to avoid filamentation. However, this will eliminate the first broad peak of the energy spread also (Fig. 11) and lead to a bigger microwave growth. Thus the actual benefit of the triple-switch scheme may not manifest itself at all.

(2) The timings $x_2$ and $x_3$ depend critically on the size of the space-charge force. Take the case of $x_2 = 0.688$ and $x_3 = 1.289$ which result in $D = 1.03$ with $\eta_0 = 1.0$. When $\eta_0$ changes to 1.25 and 0.75, $D$ becomes 1.19 and 1.14 respectively. The variation in $D$ will be much bigger when $\eta_0$ is big. Since $\eta_0$ depends on the bunch intensity which varies in each injection, thus fixing a set of $x_2$ and $x_3$ is not so beneficial.

(3) The timings $x_1, x_2$ and $x_3$ have to be rather accurate. However, Sorenssen had shown that such accuracy can be achieved during actual performance. For example, it is possible to control the timing error at transition to $\Delta x_1 \sim \pm 30\mu s$ while for the other two $\Delta x_2 \sim \Delta x_3 \sim \pm 1\mu s$. The increase in the distortion factor $D$ is only $\sim 2\%$ which is acceptable.

The triple-phase-switch method had been tried on the CERN PS without success.

## VI-2 Mechanical damping

We can devise a feed-back damper to damp out the quadrupole motion of the bunch. However, filamentation begins just after about four oscillations or $\sim$ 1.5ms. This implies that the dampling must be done within this short period which poses some technical difficulty.

## VI-3 $\gamma_t$ jump

As a bunch is approaching transition from below, if the transition gamma $\gamma_t$ is suddenly changed to a new value below the instantaneous $\gamma$ of the bunch, the bunch will not see transition at all. This method is nice because the bunch is never very near to transition, so microwave growth can be avoided to a very large extent. Secondly, away from transition, the equilibrium bunch length is not so much different from that if space charge is absent as shown in Fig. 3. Therefore, oscillations after the transition jump will generally be rather small. Last of all, $\gamma_t$ can actually be changed rather easily by pulsing some quadrupole magnets in a special way.

For the case $\dot{\gamma} = 406.5\,\mathrm{sec}^{-1}$ near transition and $T = 0.216\,\mathrm{ms}$, a transition jump of 10 units in $x$ corresponds to $\gamma_t$ changing by roughly 0.9. We can solve the equations of in Section III by letting $x_2 = 0, x_1$ negative, $x_3$ positive but $x_3 - x_1 = 10$. As soon as the integration reaches $x = x_1$, we set $x = x_3$.

As is shown in Fig. 3, the equilibrium bunch length is bigger than the bunch length without space charge below transition but smaller than the bunch length above transition. In order that the equilibrium bunch lengths before and after transition will match so as to reduce eventual oscillations as much as possible, it is beneficial to have $|x_1| < |x_3|$ or to have the transition jump performed when *the energy of the bunch is closer to the old transition energy than the new one.* The results of some computations are listed in Table 3. Some typical plots of bunch half lengths are shown in Figs. 12 and 13. It is obvious from Table 3 that the best jump should be performed at $x_2 = -4.0$ and $x_3 = 6.0$ which appear to depend very

| $x_1$ | $x_3$ | Distortion $D$ | | |
|---|---|---|---|---|
| | | $\eta_0 = 1.00$ | $\eta_0 = 0.75$ | $\eta_0 = 1.25$ |
| 0.0 | 0.0 | 1.72 | 1.55 | 1.89 |
| -5.0 | 5.0 | 1.11 | 1.08 | 1.14 |
| -4.5 | 5.5 | 1.07 | 1.05 | 1.10 |
| -4.0 | 6.0 | 1.03 | 1.02 | 1.05 |
| -3.5 | 6.5 | 1.05 | 1.07 | 1.02 |
| -3.0 | 7.0 | 1.09 | 1.12 | 1.06 |
| -2.5 | 7.5 | 1.14 | 1.18 | 1.11 |
| -2.0 | 8.0 | 1.21 | 1.25 | 1.17 |
| -1.5 | 8.5 | 1.31 | 1.36 | 1.26 |
| -1.0 | 9.0 | 1.40 | 1.46 | 1.34 |

Table 3: Distortions for a transition jump of $\Delta\gamma_t \sim 0.9$ for various space-charge strengths and jumping at different time.

weakly on the space-charge strength. Translating to the actual time units, if we want to perform a transition jump from $\gamma_t = 5.37$ to 4.47, the best time to make the jump is when the bunch is $4.0 \times 0.216 = 0.86$ ms before the original transition time or when the bunch has a $\gamma$ of $5.37 - 0.86 \times 10^{-3} \times 406.5 = 5.02$.

# VII Conclusion

We have studied the space-charge effects on a bunch across transition. Since the RF potential has been linearized, the bunch area becomes a constant and no microwave growth has been included. However, the tumbling of the bunch after transition agrees very well with the measurements indicating that impedance of other sources and microwave instability are of minor importance here. $\gamma_t$ jump has been investigated in order to cure the bunch tumbling. This is the most ideal method to reduce tumbling. We find that, in order to achieve the best tumbling suppression, the timing of the transition jump should be tuned to a point where the energy of the bunch is closer to the old transition energy than the new one.

# References

[1] J. Crisp, Fermilab Director Review (1986).

[2] A. Sorenssen, CERN Report MPS/Int. MU/EP 67-2 also Particle Accelerators **6**, 141 (1975).

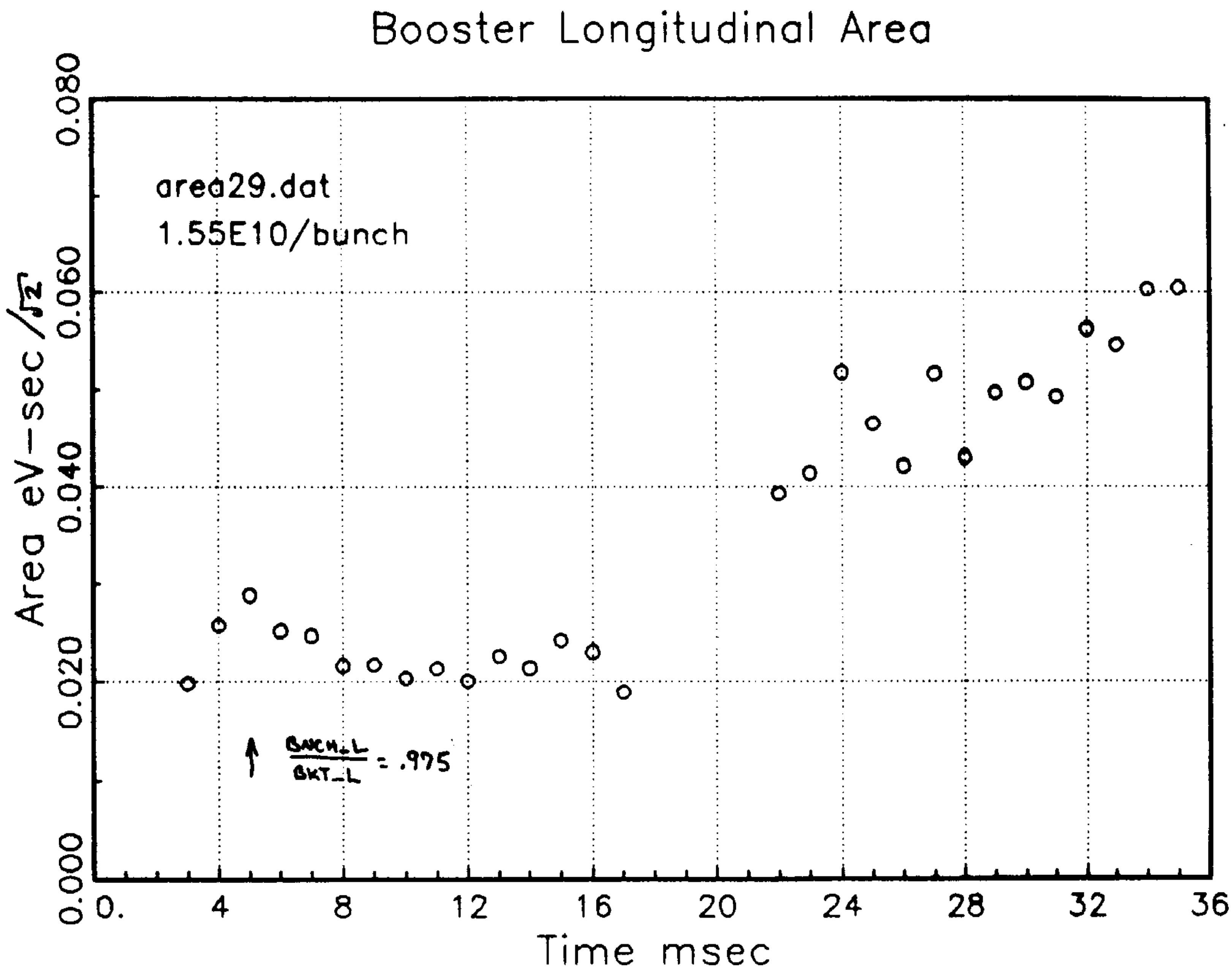
Booster Longitudinal Area
area29.dat
1.55E10/bunch
BNCH_L / BKT_L = .975
Area eV-sec/√2
0.000
0.020
0.040
0.060
0.080
0.
4
8
12
16
20
24
28
32
36
Time msec

Figure 1

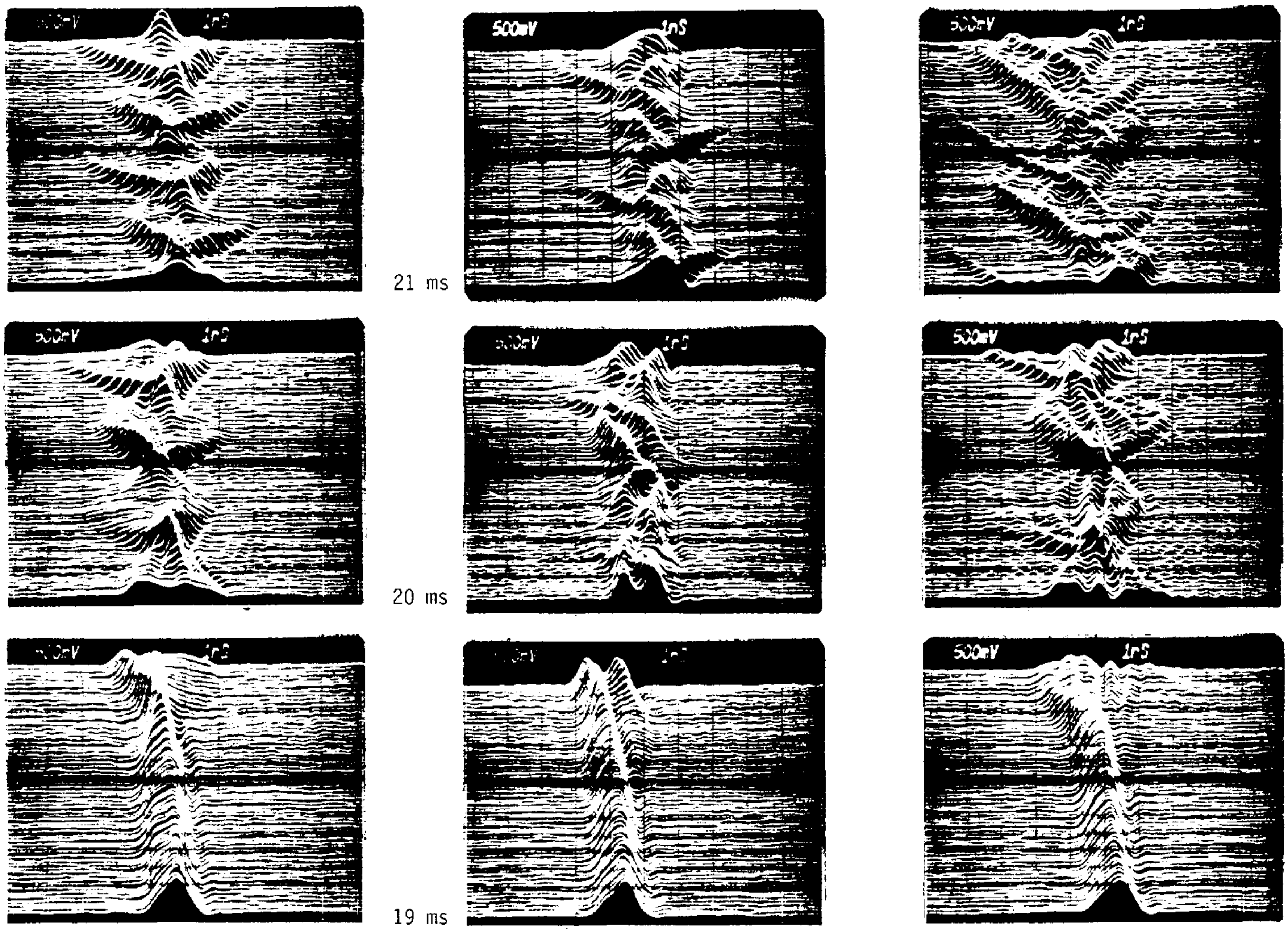


RF phase switched at 19.355 ms (right at transition)

RF phase switched at 19.555 ms

RF phase switched at 19.755 ms

Figure 2

Figure 3

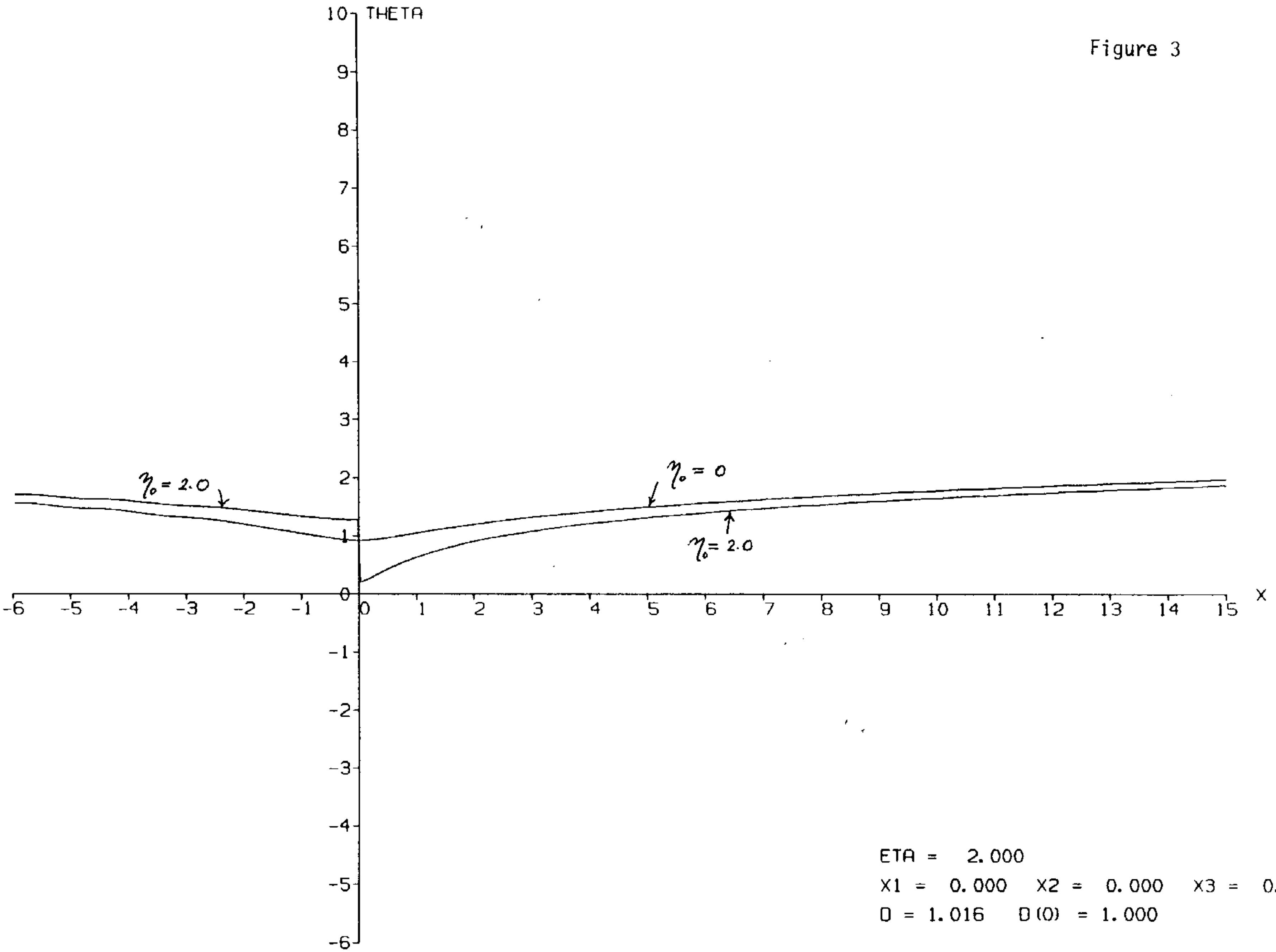


ETA = 2.000
X1 = 0.000 X2 = 0.000 X3 = 0.000
D = 1.016 D(0) = 1.000

Figure 4

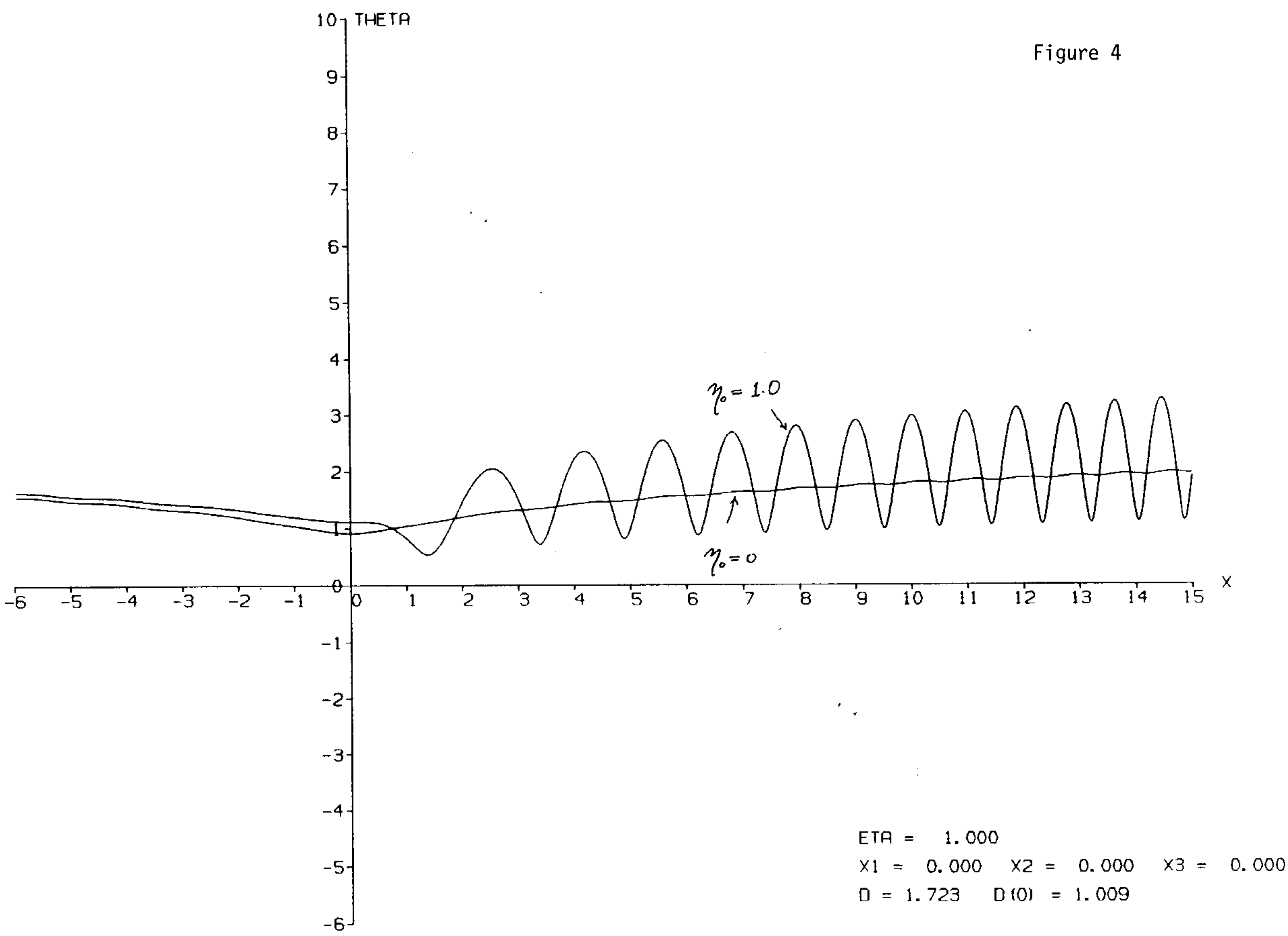
THETA
X
$\eta_o = 1.0$
$\eta_o = 0$
ETA = 1.000
X1 = 0.000 X2 = 0.000 X3 = 0.000
D = 1.723 D(0) = 1.009

Figure 5

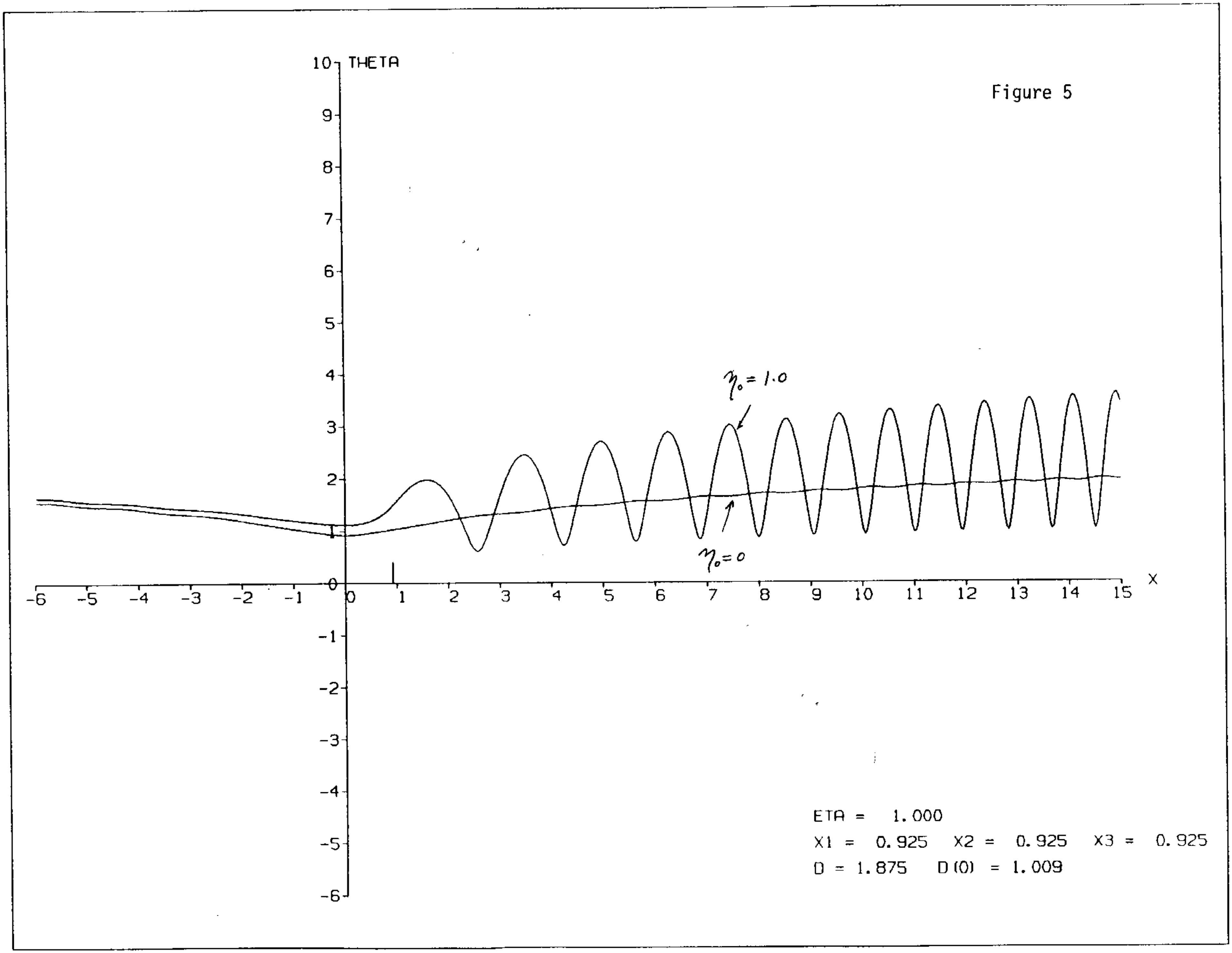

THETA
X
$\eta_0 = 1.0$
$\eta_0 = 0$
ETA = 1.000
X1 = 0.925 X2 = 0.925 X3 = 0.925
D = 1.875 D(0) = 1.009

Figure 6

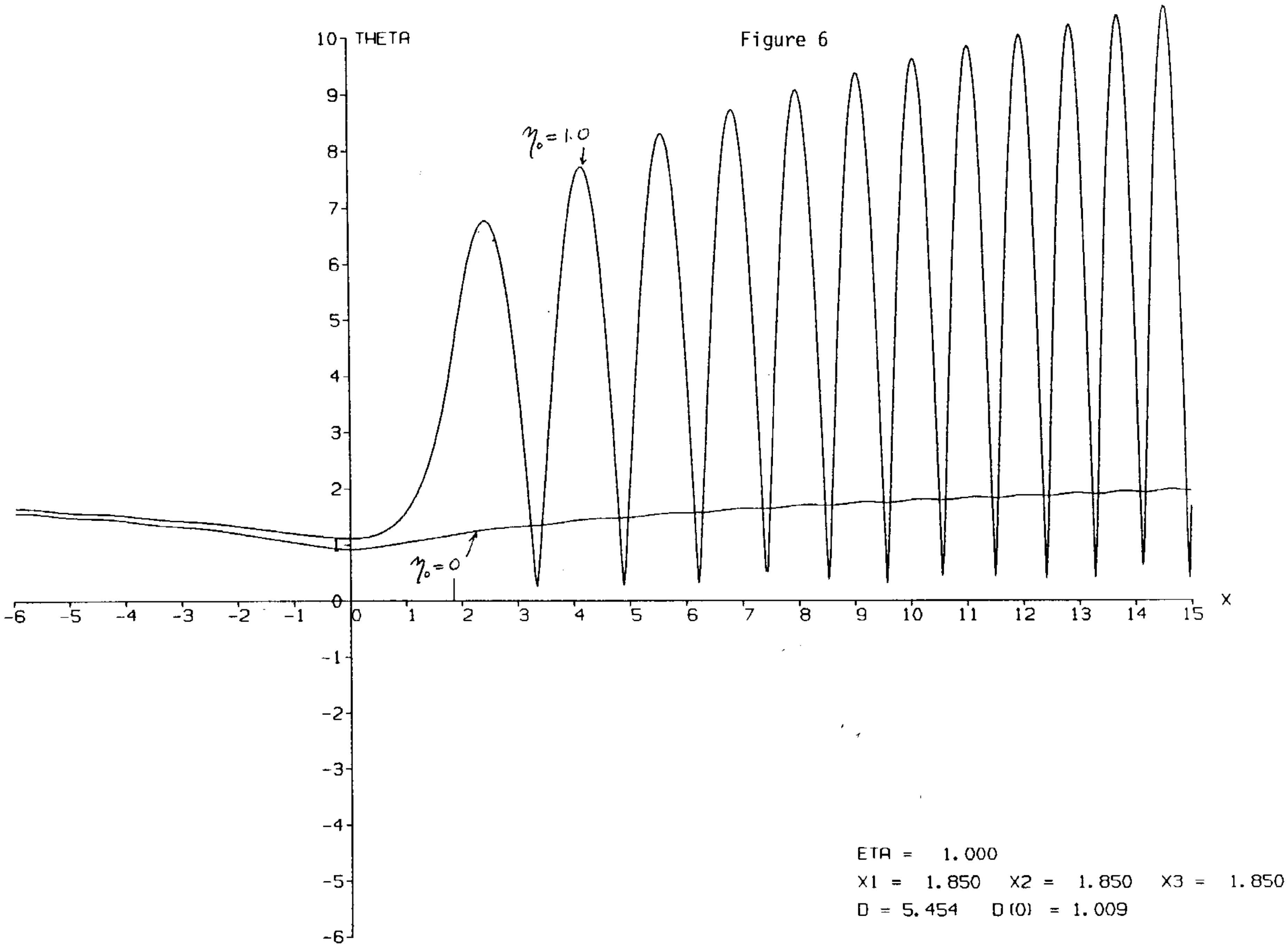
THETA
X
$\eta_0 = 1.0$
$\eta_0 = 0$
ETA = 1.000
X1 = 1.850 X2 = 1.850 X3 = 1.850
D = 5.454 D(0) = 1.009

Figure 7

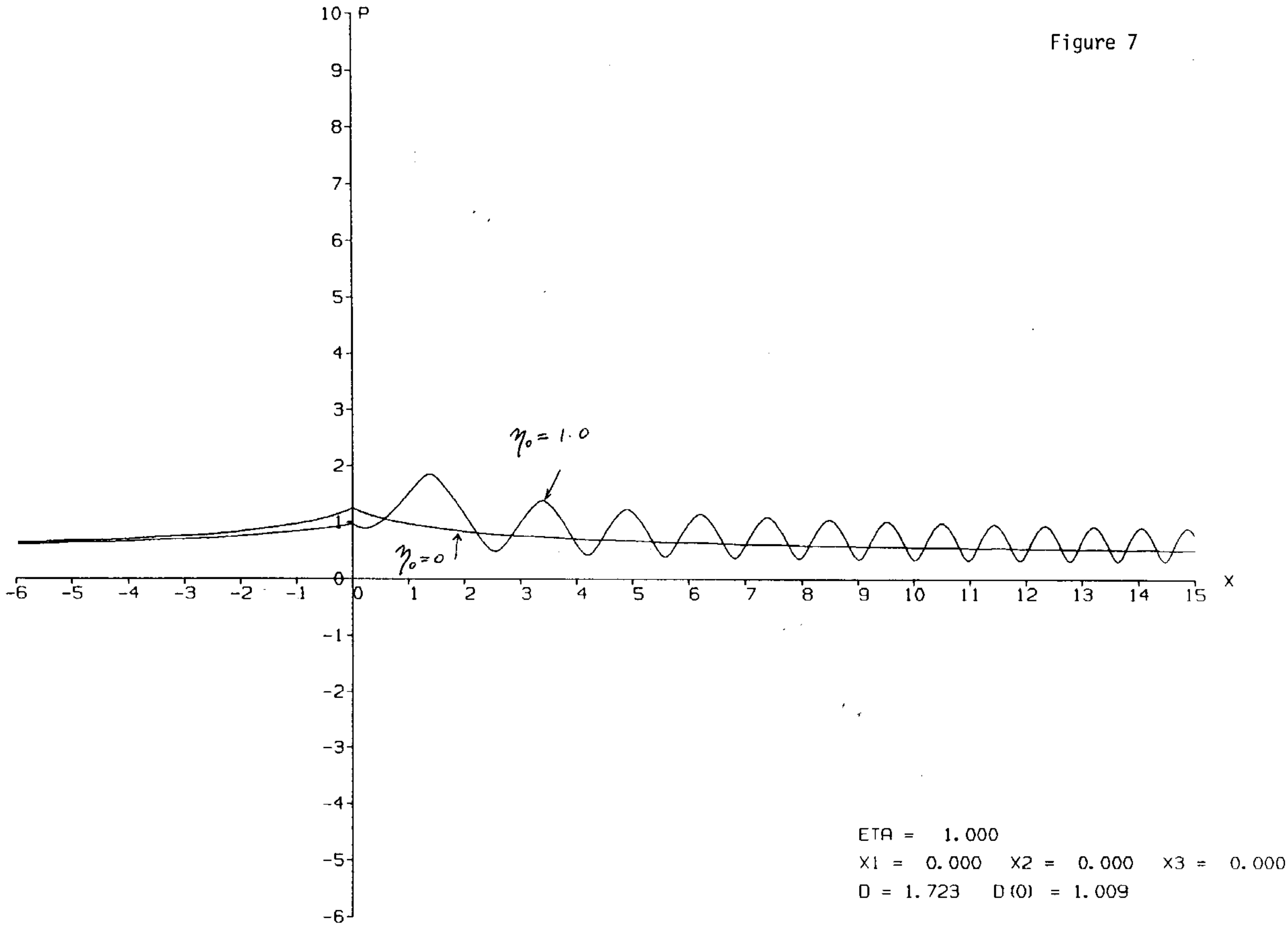

P
10
9
8
7
6
5
4
3
2
1
0
-1
-2
-3
-4
-5
-6
X
-6 -5 -4 -3 -2 -1 0 1 2 3 4 5 6 7 8 9 10 11 12 13 14 15
$\eta_o = 1.0$
$\eta_o = 0$
ETA = 1.000
X1 = 0.000 X2 = 0.000 X3 = 0.000
D = 1.723 D(0) = 1.009

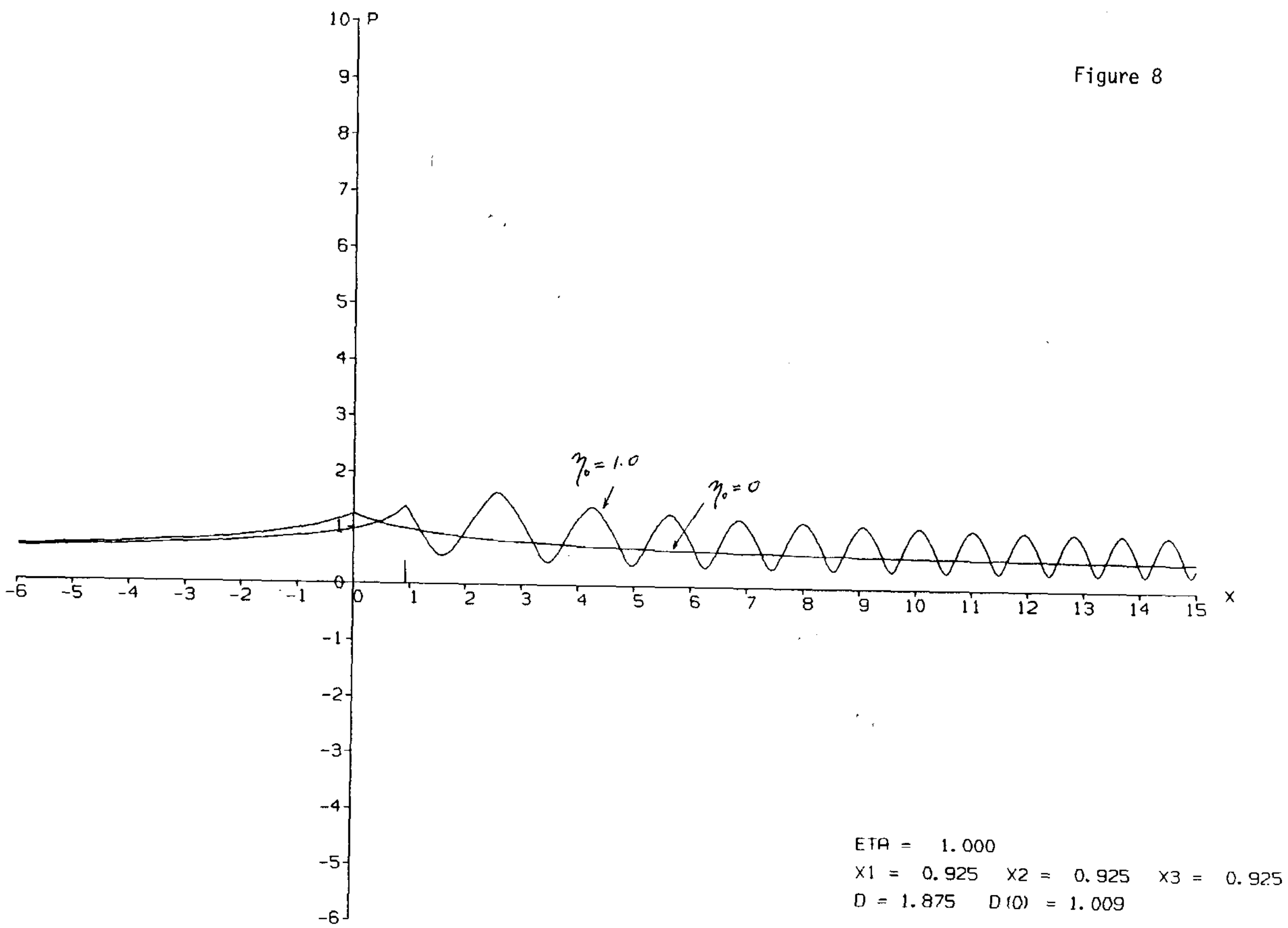


Figure 8

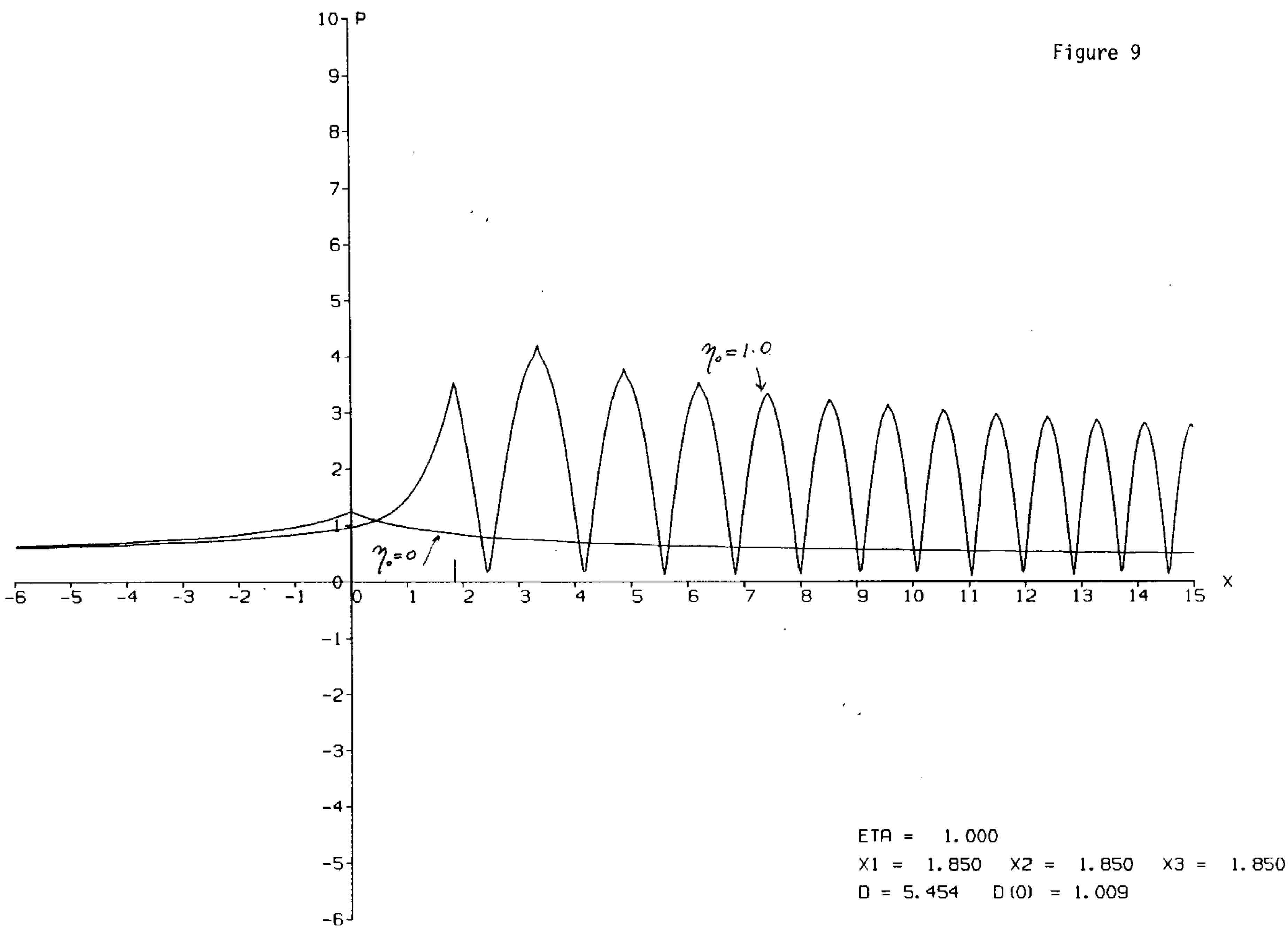


Figure 9

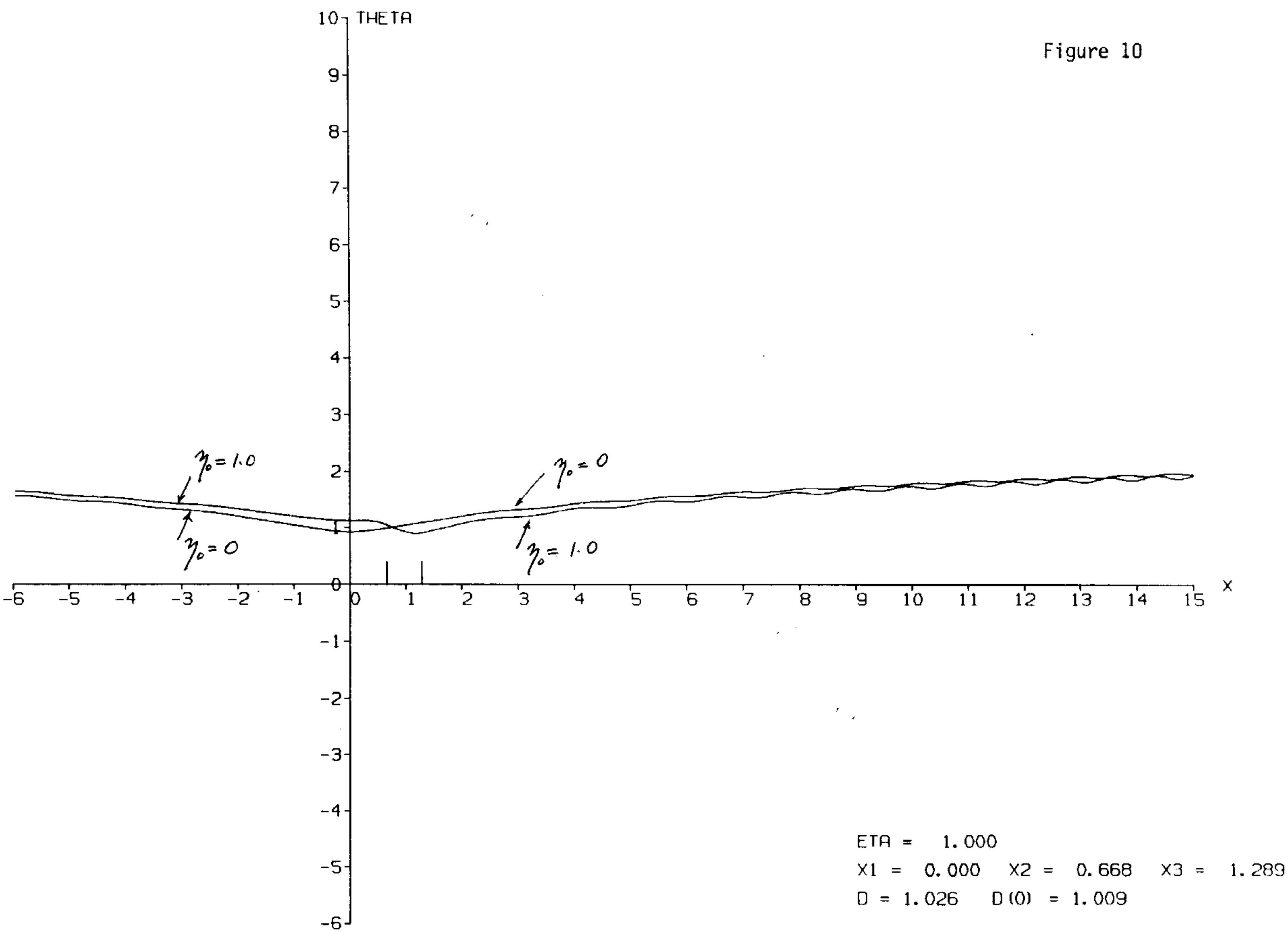
10
9
8
7
6
5
4
3
2
1
0
-1
-2
-3
-4
-5
-6
THETA
X
-6 -5 -4 -3 -2 -1 0 1 2 3 4 5 6 7 8 9 10 11 12 13 14 15
$\eta_o = 1.0$
$\eta_o = 0$
$\eta_o = 0$
$\eta_o = 1.0$
ETA = 1.000
X1 = 0.000 X2 = 0.668 X3 = 1.289
D = 1.026 D(0) = 1.009

Figure 10

Figure 11

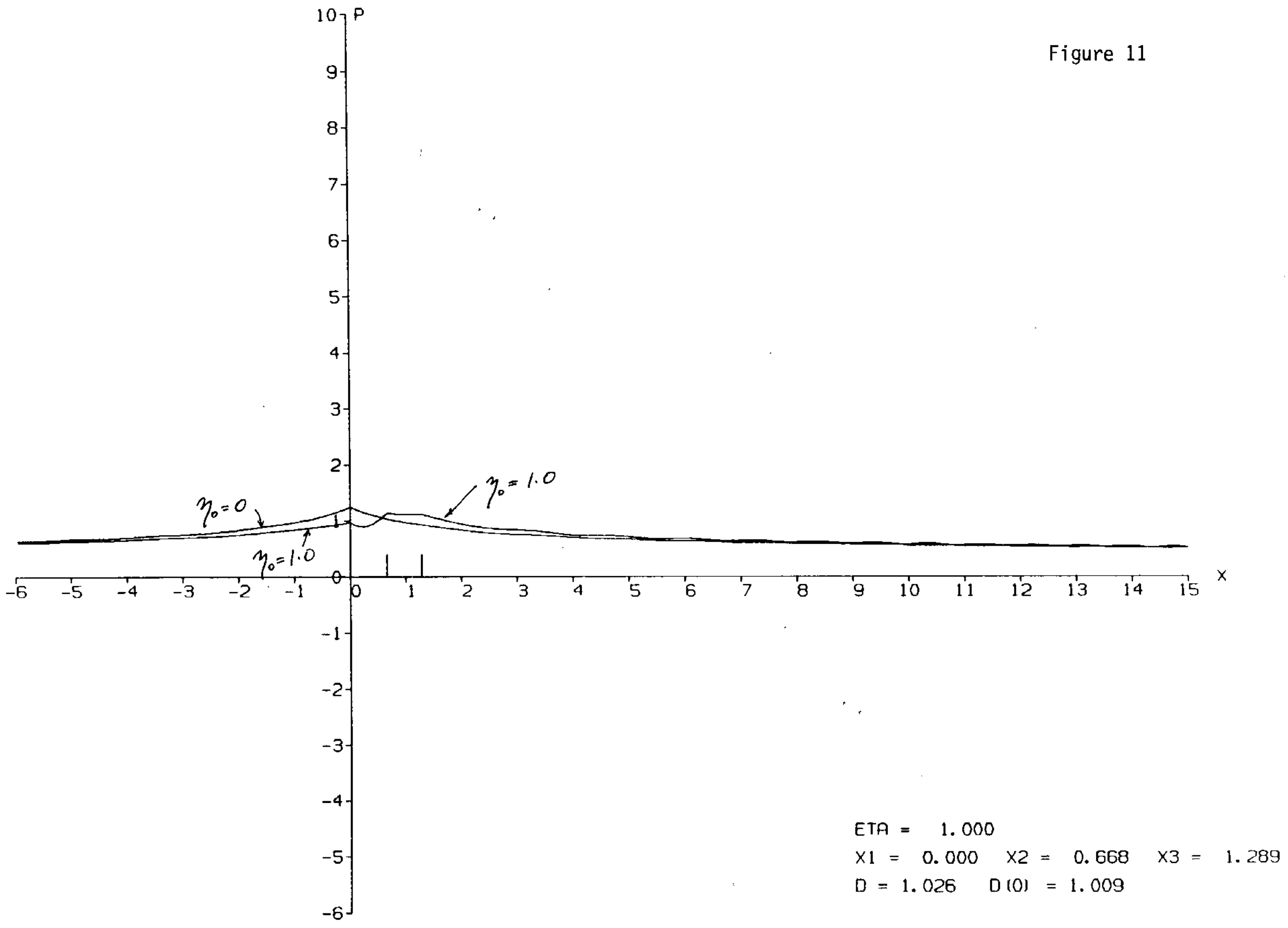

P
X
$\eta_0 = 0$
$\eta_0 = 1.0$
$\eta_0 = 1.0$
ETA = 1.000
X1 = 0.000 X2 = 0.668 X3 = 1.289
D = 1.026 D(0) = 1.009

Figure 12

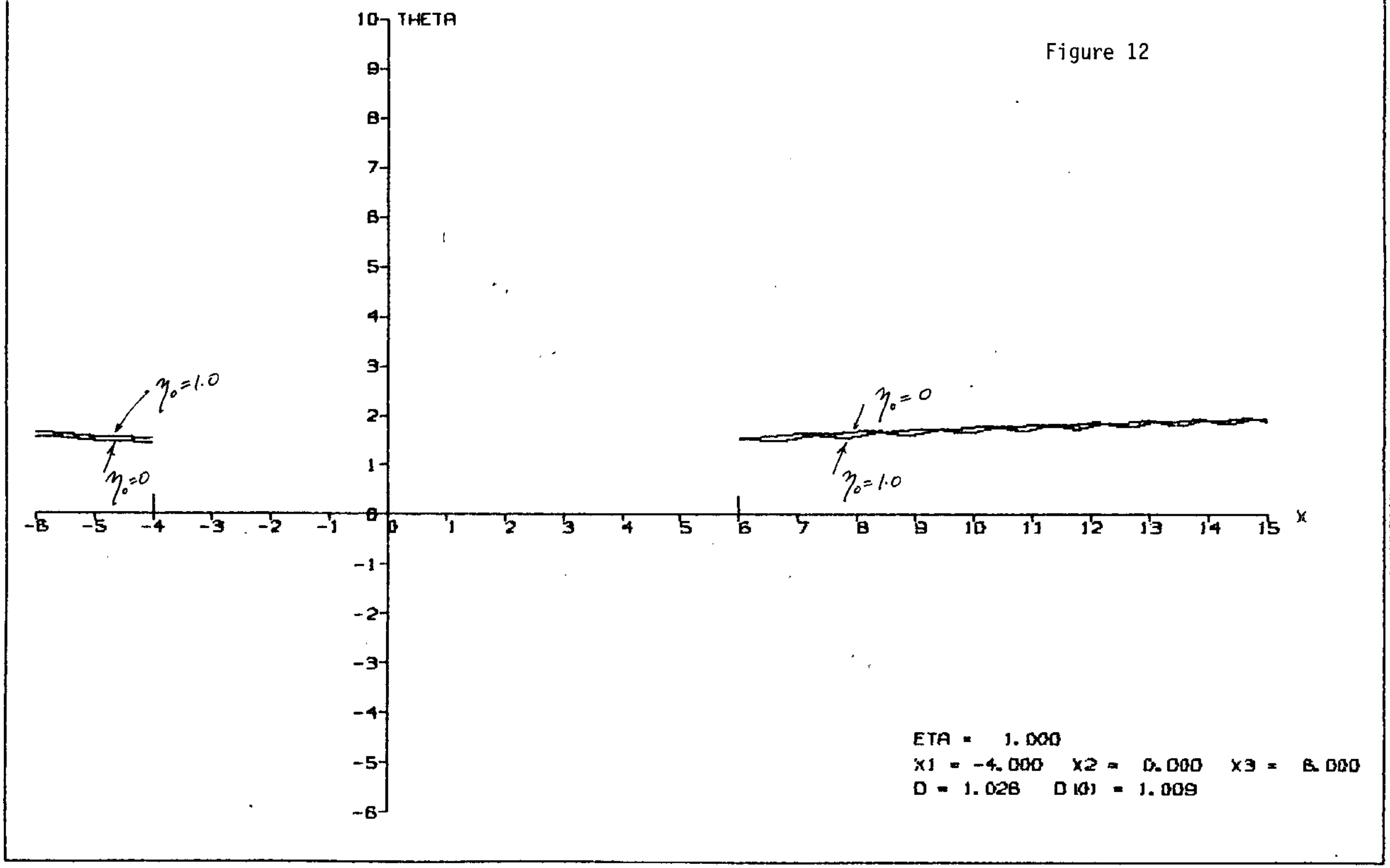
THETA
X
$\eta_0=1.0$
$\eta_0=0$
$\eta_0=0$
$\eta_0=1.0$
ETA = 1.000
X1 = -4.000 X2 = 0.000 X3 = 6.000
D = 1.026 D(0) = 1.009

Figure 13

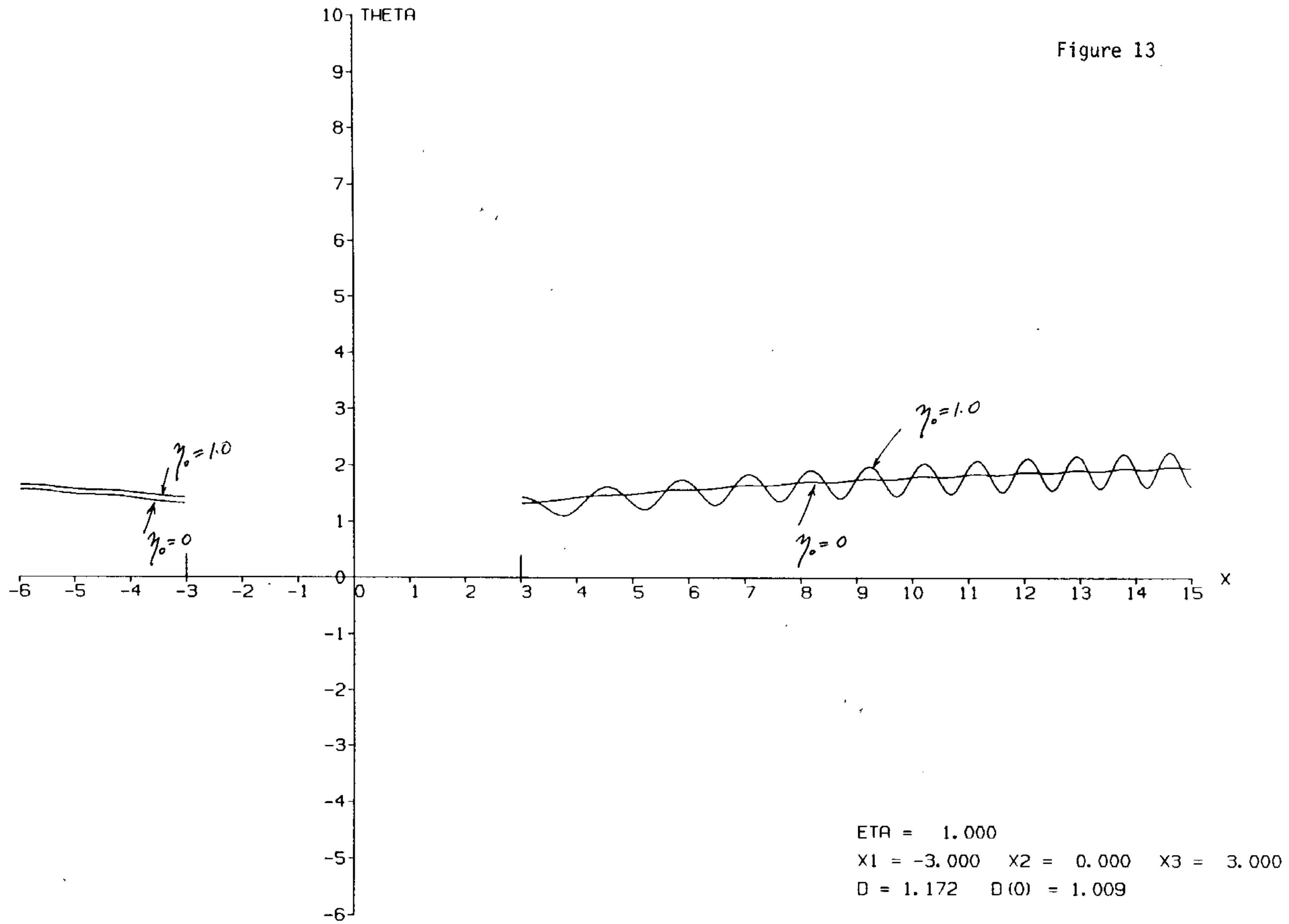
THETA
X
$\eta_0 = 1.0$
$\eta_0 = 0$
$\eta_0 = 1.0$
$\eta_0 = 0$
ETA = 1.000
X1 = -3.000 X2 = 0.000 X3 = 3.000
D = 1.172 D(0) = 1.009